Journal of Colloid and Interface Science 364 (2011) 417–427

Contents lists available at SciVerse ScienceDirect

Journal of Colloid and Interface Science

www.elsevier.com/locate/jcis

Computational studies on the behavior of Sodium Dodecyl Sulfate (SDS) at TiO_2(rutile)/water interfaces

Edgar Núñez-Rojas *, Hector Domínguez

Instituto de Investigaciones en Materiales, UNAM, Universidad Nacional Autónoma de México, México D.F. 04510, Mexico

ARTICLE INFO

Article history:
Received 2 July 2011
Accepted 26 August 2011
Available online 2 September 2011

Keywords:
Computer simulations
SDS surfactant
Adsorption
Rutile

ABSTRACT

Molecular dynamics simulations to study the behavior of an anionic surfactant close to TiO_2 surfaces were carried out where each surface was modeled using three different crystallographic orientations of TiO_2 (rutile), (001), (100) and (110). Even though all three surfaces were made with the same atoms the orientation was a key to determine adsorption since surfactant molecules aggregated in different ways. For instance, simulations on the surface (100) showed that the surfactant molecules formed a hemicylinder structure whereas the molecules on the surface (110) were attached to the solid by forming a hemisphere-like structure. Structure of the aggregated molecules and surfactant adsorption on the surfaces were studied in terms of tails and headgroups density profiles as well as surface coverage. From density profiles and angular distributions of the hydrocarbon chains it was possible to determine the influence of the solid surface. For instance, on surfaces (100) and (001) the surfactant molecules formed molecular layers parallel to the surface. Finally, it was found that in the solids (100) and (110) where there are oxygen atoms exposed on the surface the surfactant molecules were attached to the surfaces along the sites between the lines of these oxygen atoms.

1. Introduction

Adsorption of surfactant molecules at solid–liquid interfaces has been studied for many years due to the importance in several industrial processes such as corrosion inhibition, dispersion stabilization, detergency, crude oil refining, treatment of waste water, adsorption on activated charcoal and even in pharmaceutical preparations where surfactant molecules are used to stabilize solid ingredients dispersed in water [1–3]. In general, dispersion of solid particles in aqueous media is a process which takes advantage of amphiphilic properties of surfactant molecules. Moreover, understanding self-aggregation will help us not only to improve these important industrial processes but also will help us to provide fundamental physical insight of general self-assembly processes [4,5].

On the other hand, adsorption of surfactant molecules on solid surfaces has shown different issues from those observed at liquid/vapor and at liquid/liquid interfaces. For instance, changes in the slopes of the isotherms have been observed before the systems reach critic micellar concentration (CMC). These changes in slopes depend on the interactions between hydrophobic tails, repulsions between headgroups and interactions between surfactant molecules with the solid surface [6,7].

Nowadays, adsorption and structures on surfaces have been studied by different experimental techniques such as streaming potential methods [8], calorimetry [9], neutron reflection [10], ellipsometry [11], fluorescence spectroscopy [12] and atomic force microscopy (AFM) [13]. In fact, by AFM people have obtained detailed information about the topology of aggregation of surfactants, e.g. Manne et al. observed the self-assembling of CTAB molecules on a surface of graphite in parallel stripes [14] and similar morphologies have been seen for other surfactants on hydrophobic surfaces [15–17]. Recently, Schniepp et al. were able to obtain high resolution images of SDS aggregates on a rough gold surface where they reported a hemimicelle morphology which depended on the local curvature of the surface [18].

For these studies, different solid surfaces have been used as substrates such as graphite, gold, mica, etc. however, studies on titanium dioxide (TiO_2) surfaces have also been conducted. For instance, proteins adsorbed on TiO_2 to be used as biosensors have been investigated [19], besides, studies in assembly of materials in electronic devices due to the electronic conduction properties of titania have been carried out [20]. On the other hand, the interaction of different surfactant molecules with TiO_2 has been studied in order to determine adsorption and some factors involved on this phenomenon [21–24]. In fact, among various semiconductor materials, TiO_2 has attracted much interest due to its potential use in industry [25,26]. Moreover, surfaces of rutile have been subject of few studies from both experimental and theoretical points of

* Corresponding author.
E-mail addresses: eeddgar@yahoo.com.mx (E. Núñez-Rojas), hectordc@servidor.unam.mx (H. Domínguez).

0021-9797/$ - see front matter © 2011 Elsevier Inc. All rights reserved.
doi:10.1016/j.jcis.2011.08.069

view [27,28]. Experimentally people have investigated three different orientations, (001), (100) and (110) [29] and by conducting studies of contact angles of drops of water on these surfaces they found different hydrophobicities; the surfaces (110) and (001) were the most hydrophobic ones, however, the surface (100) showed a smaller hydrophobicity than that in graphite.

From a computational perspective several studies have been conducted to study molecular aggregation, for instance, Coarse-grained Monte Carlo investigations have provided useful information about morphological transitions of surfactant surface aggregation [30] while molecular dynamics simulations have been carried out to investigate aggregate properties at atomistic scales [31,32]. Monolayers and their dynamics on a graphite surface have been also studied and it was found that graphite surfaces impose an orientational bias the carbon atoms in the solid and for the surfactant–solid interactions [32].

In previous papers the interaction of SDS molecules on graphite surfaces has been investigated where hemicylinder structures were reported. In the present paper we are now interested to extent the studies of the structural analysis of the same surfactant molecule in a different surface (rutile). Moreover, we focus in how different crystallographic orientations of the solid modify the surfactant structure on the surface.

2. Computational method and model

For the present study molecular dynamics simulations of surfactant molecules at three different rutile surfaces were carried out. The surfaces were constructed using an atomistic model for the three surface orientations (Fig. 1).

Fig. 1a is the surface (001), Fig. 1b is the surface (100) and Fig. 1c is the surface (110) where it is possible to see they have different structural array of atoms. In particular surfaces (100) and (110) have oxygen atoms exposed on the top of the solid surface whereas as in the surface (001) we observed that oxygen and titanium atoms are both on the surface of the solid. For the surfactant molecule we used a Sodium Dodecyl Sulfate (SDS) model of 12 united carbon atoms attached to a headgroup, SO_4, where the headgroup atoms were explicitly modeled. The initial configuration was prepared from a monolayer of 36 surfactant molecules in all-trans configuration with the SDS headgroups initially pointed to the solid surface and placed close to the rutile surface. Then 2535 water molecules were added (using the SPC model [33]) to the system and 36 sodium cations (Na^+) were also included close to the headgroups. The concentration of surfactant molecules was chosen to be similar to the critical micelle concentration area for SDS molecules at the water/vapor interface, as found in neutron reflection experiments [34]. The number of molecules corresponded to a high concentration used in real experiments, however, with this number we guaranteed that aggregation was observed in the present simulations.

The usual periodic boundary conditions were imposed in the simulations, however, the z-dimension of the box was set to 150 Å. This length was long enough to prevent the formation of a second water/solid interface due to the periodicity of the system. Instead, a liquid/vapor interface was present at one end of the box ($z > 0$) whereas at the other end of the box ($z > 0$) beyond the solid was an empty space. The simulation parameters for the solid surface and the SDS molecules were taken from previous works [35,36] and they were summarized in Tables 1 and 2. All simulations were carried out in the NVT ensemble with a time step of 0.002 ps using DL-POLY package [37]. Bond lengths were constrained using SHAKE algorithm with a tolerance of 10^{-4} and the temperature was controlled using the Hoover–Nose thermostat with a relaxation time of 0.2 ps [38] at $T = 298$ K. The long-range

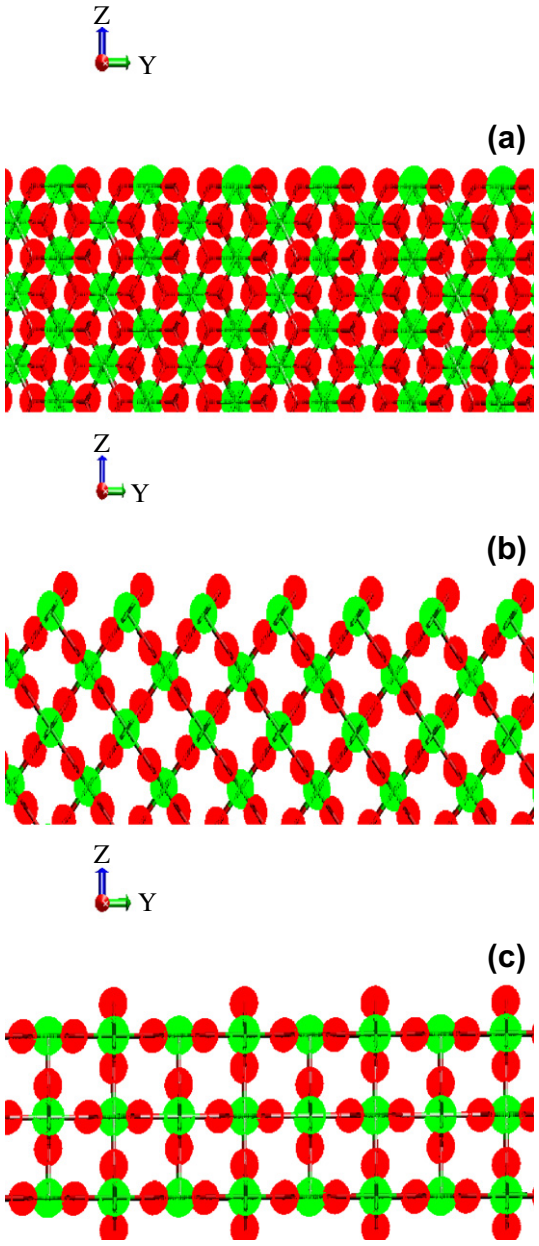

Fig. 1. Structures of solid surfaces of rutile. Oxygen atoms are red balls and titanium atoms are green balls. (a) Solid surface with (001) orientation, (b) solid surface with (100) orientation, (c) solid surface with (110) orientation. (For interpretation of the references to color in this figure legend, the reader is referred to the web version of this article.)

electrostatic interactions were handled with the Particle Mesh Ewald method, and the Van der Waals interactions were cut off at 10 Å. Finally, all simulations were run up to 40 ns and configurational energy was monitored as a function of time to determine when systems reached equilibrium. Then, we collected data from the last 2 ns for analysis. A typical simulation took around 24 h to run 1 ns in a AMD processor in a computer with 8 nodes. In Table 3 dimensions of the solid walls and number of TiO_2 molecules used to build them are shown.

The total intramolecular potential for the surfactant included bond, angular and torsional potentials,

$$E = E_{bond} + E_{ang} + E_{tor} \quad (1)$$

The bond lengths were modeled by an harmonic potential,

Table 1
intramolecular SDS potential parameters.

Sodium Dodecyl Sulfate			
Group	K_{ang} (kcal/mol rad^2), θ_0 (rad)	Torsion, A (kcal/mol), δ (rad), m	K_{bond} (kcal/mol Å^2), r_0 (Å^2)
CH_n–CH_n–CH_n	124.3, 111.0		
CH_n–CH_n–O(ester)	124.3, 109.5		
CH_n–O(ester)–S	124.3, 112.6		
O(ester)–S–O	102.0, 102.6		
O–S–O	102.0, 115.4		
CH_n–CH_n–CH_n–CH_n		R–B[a]	
CH_nCH_n–CH_n–O(ester)		1.000, 0, 3, cos	
CH_3CH_2–O(ester)–S		0.725, 0, 3, cos	
CH_2–O(ester)–S–O		0.250, 0, 3, cos	
CH_2–CH_2			620.0, 1.53
C–O(ester)			600.0, 1.42
O(ester)–S			600.0, 1.58
S–O			900.0, 1.46

[a] R–B (kcal/mol) $C_0 = 2.218$, $C_1 = 2.906$, $C_2 = -3.136$, $C_3 = -0.731$, $C_4 = 6.272$, $C_5 = -7.528$.

Table 2
LJ intermolecular potential parameters.

Sodium Dodecyl Sulfate			
Site	q (charge)	σ (Å)	ϵ (kcal/mol)
S	1.284	3.550	0.250
$O(SO_3)$	−0.654	3.150	0.200
O(ester)	−0.459	3.000	0.170
CH_2 (attached to O)	0.137	3.905	0.118
CH_2	0.000	3.905	0.118
CH_3	0.000	3.905	0.175
Na^+	1.000	2.275	0.115
Water and TiO_2			
OW (H_2O)	−0.82	3.166	0.155
HW (H_2O)	0.41	1.782	0.000
Ti (TiO_2)	1.15	3.788	0.40811
O (TiO_2)	−0.575	3.627	0.18676

Table 3
Spatial dimensions and number of molecules used to build the solid surfaces.

Plane	L_x (Å)	L_y (Å)	L_z (Å)	Molecules of TiO_2
(001)	42.2394	42.2394	11.8348	729
(100)	42.9011	42.2394	8.2913	504
(110)	39.9424	40.2461	12.9929	702

$$E_{bond} = K_b(r - r_0)^2 \tag{2}$$

where r_0 is the equilibrium distance between two bonded atoms and K_b is the bond constant. The angles in the chain were also constrained by an harmonic potential,

$$E_{ang} = K_\theta(\theta - \theta_0)^2 \tag{3}$$

where θ_0 is the equilibrium angle and K_θ is the force constant. The torsional angles were modeled by the Ryckeart and Bellemans (R–B) potential [39] for the tails whereas a cosine potential form was used for the headgroup (see Table 1),

$$E_{tor-cos} = A[1 + cos(m\phi - \delta)] \tag{4}$$

$$E_{tor-RB} = \sum_{k=0}^{5} c_k cos^k(\phi) \tag{5}$$

where the c_k are the energy constants and ϕ is the dihedral angle. The potential parameters are given in Table 1.

3. Results

In this section we present the calculations performed on the SDS surfactant on the three different rutile surfaces. Studies on the behavior of the SDS molecules and how they aggregated at the liquid/solid interfaces are discussed.

3.1. Density profiles

In order to see where the surfactant molecules arrayed in the system mass Z-depended density profiles for the headgroups and the tails were calculated, i.e. normal to the liquid/solid interface.

Fig. 2 shows the density profiles calculated along the z-direction for the surfactant molecules interacting with the solid surface (001). From this figure we observed a layer of SDS molecules on the surface attached by their hydrophobic tails (first peak of the solid line in the density profile).

Moreover, it was also possible to depict the formation of a second and a third layer of tailgroups. A snapshot of the final configuration of this simulation is shown in Fig. 3.

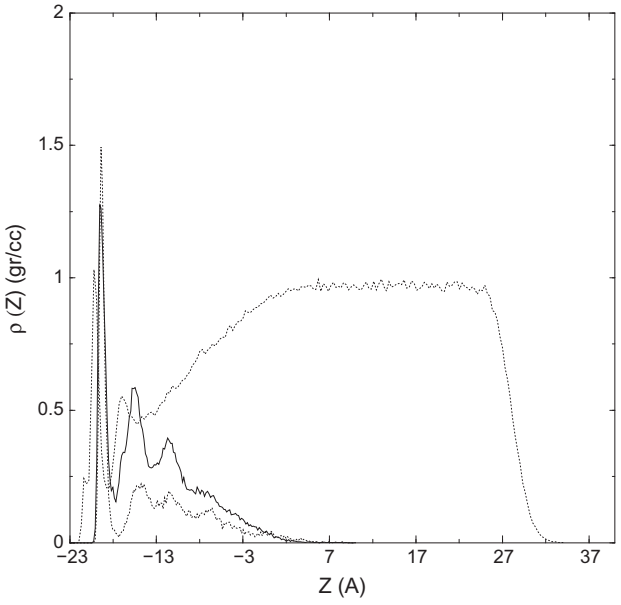

Fig. 2. Z-density profile for the system with the solid surface (001). The dotted line represents water, the dashed line the headgroups and the solid line the tailgroups of the surfactant molecules. The solid surface is located at the left of the plot.

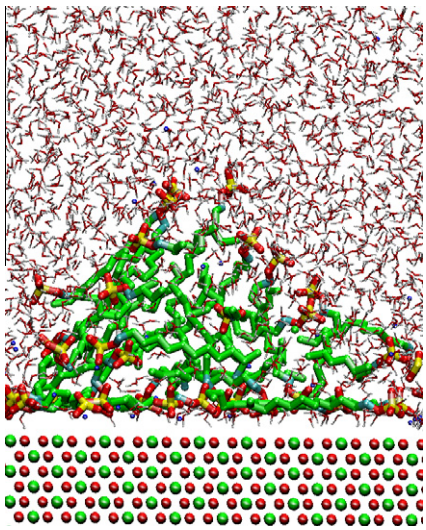

Fig. 3. Snapshot of the final configuration of the SDS molecules on the solid surface (001). Yellow balls with four surrounding red balls correspond to the headgroups. Green balls correspond to the tailgroups. (For interpretation of the references to color in this figure legend, the reader is referred to the web version of this article.)

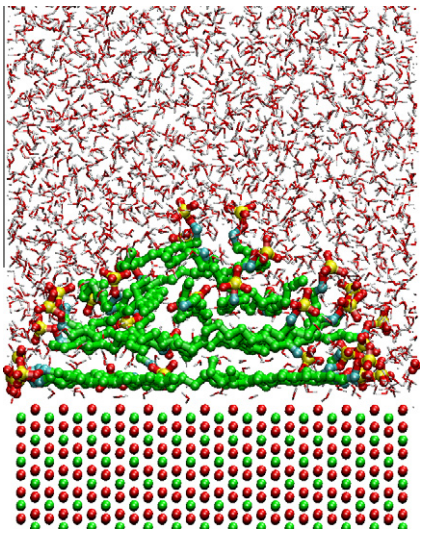

Fig. 5. Snapshot of the final configuration of the SDS molecules on the solid surface (100). The colors are the same as in Fig. 3. (For interpretation of the references to color in this figure legend, the reader is referred to the web version of this article.)

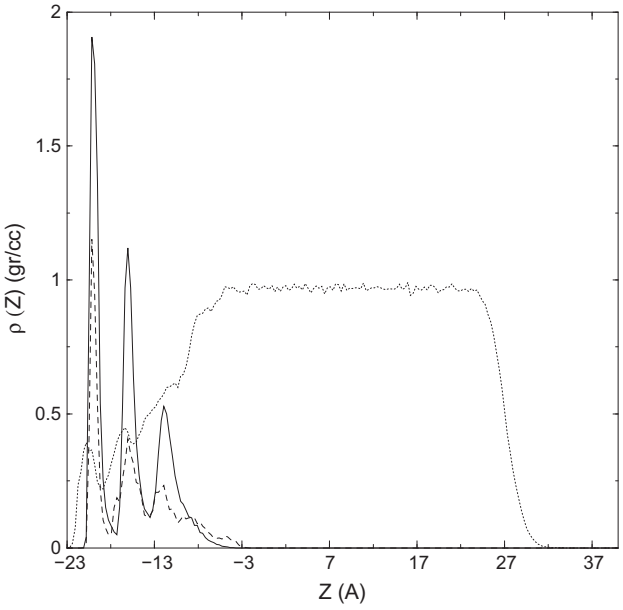

Fig. 4. *Z*-density profile for the system with the solid surface (100). The dotted line represents water, the dashed line the headgroups and the solid line the tailgroups of the surfactant molecules. The solid surface is located at the left of the plot.

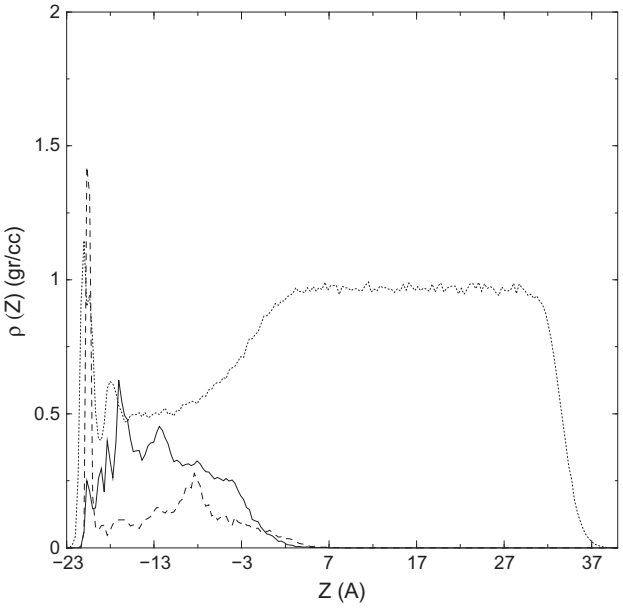

Fig. 6. *Z*-density profile for the system with the solid surface (110). The dotted line represents water, the dashed line the headgroups and the solid line the tailgroups of the surfactant molecules. The solid surface is located at the left of the plot.

Fig. 4 shows the density profiles of SDS molecules on the solid surface (100). Although a similar behavior was observed of that on the surface (001) in this case the profiles shown strong peaks suggesting that the SDS molecules arrayed in well defined layers parallel to the surface. In Fig. 5 a snapshot of the final configuration of the SDS molecules on this solid surface is shown.

The density profiles of the SDS molecules on the surface (110) are shown in Fig. 6. In that figure a different behavior to that observed in the solid surfaces (001) and (100) was depicted, i.e. the surfactant molecules were not attached to the surface by the tails. In this case the molecules near to the surface were adsorbed by their polar groups as indicated by the strong peak of the headgroup profile (dashed line in Fig. 6). This result suggested that this surface was not as hydrophobic as the (001) or the (100). Besides, the headgroup density profile also suggested the formation of a different aggregate structure adsorbed on the solid surface indicated by the shape of the final configuration of the system (see Fig. 7).

3.2. Structural analysis of molecules adsorbed on the solid surfaces

It was also possible to analyze the structure of the surfactant molecules directly from the configurations of the systems.

For instance, Fig. 8 shows snapshots of the last positions of the surfactant molecules projected into the *XZ* (Fig. 8a) and *XY* planes (Fig. 8b) on the surface (001). Although, it was possible to observe the SDS tails on the surface it was hard to associate any structure.

On the other hand, the configuration of the SDS molecules on the solid surface (100) indicated that molecules formed a hemicylinder shape attached to the solid surface (with the headgroups

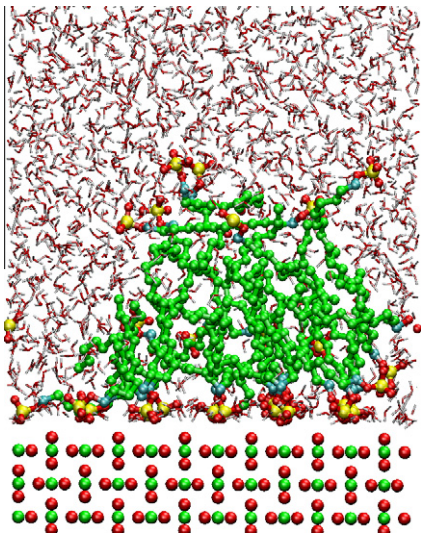

Fig. 7. Snapshot of the final configuration of the SDS molecules on the solid surface (1 1 0). The colors are the same as in Fig. 3. (For interpretation of the references to color in this figure legend, the reader is referred to the web version of this article.)

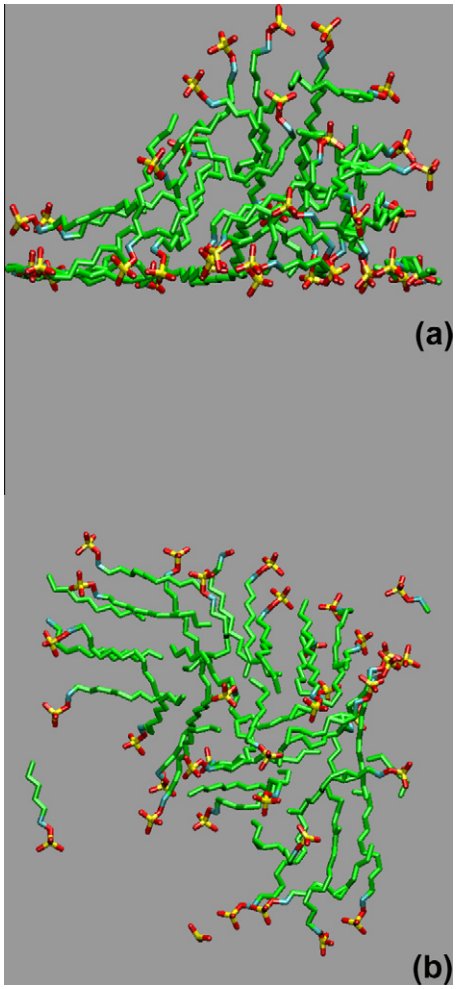

Fig. 8. Snapshot of surfactant molecules on the solid surface (0 0 1). (a) Snapshot in the *ZX* plane; (b) snapshot in the *XY* plane. The snapshots did not show any structure for this system. The colors are the same as in Fig. 3. (For interpretation of the references to color in this figure legend, the reader is referred to the web version of this article.)

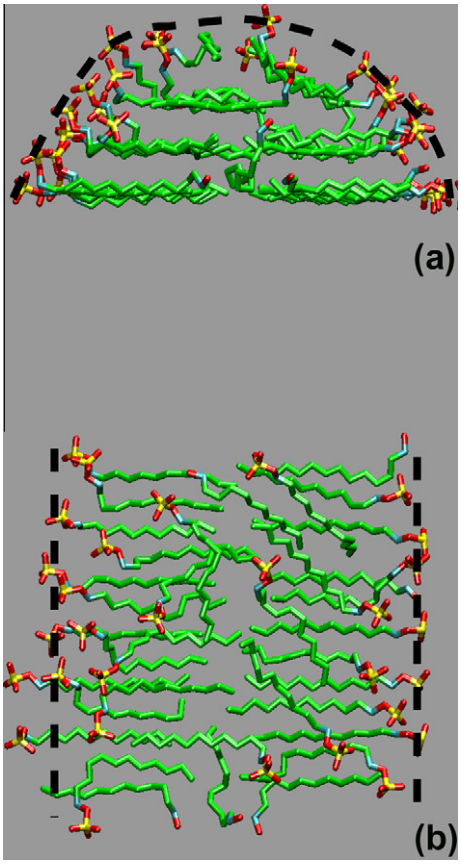

Fig. 9. Snapshot of surfactant molecules on the solid surface (1 0 0). (a) Snapshot in the *ZX* plane; (b) snapshot in the *XY* plane. The black dashed lines are a guide to see the approximated structure. The colors are the same as in Fig. 3. (For interpretation of the references to color in this figure legend, the reader is referred to the web version of this article.)

located on the surface of the hemicylinder) as suggested by the configurations projected into the *XZ* and *XY* planes (Fig. 9). Therefore, by using geometric parameters it was possible to fit a hemicylinder to several configuration at different times and we calculated an average contact angle of the aggregate with the surface. The contact angle obtained was ≈68°.

A similar value was found in simulations of SDS on graphite where a contact angle of 60° was calculated [40].

Fig. 10 shows a snapshot of the final configuration of the SDS molecules on the solid surface (1 1 0). In this figure it was possible to see that surfactant molecules formed a structure which it was surrounded with the headgroups, i.e. the structure in this case looked like as an hemisphere as it was shown in Fig. 10a (*XZ* plane) and Fig. 10b (*XY* plane). Then, once more, by using geometric parameters we calculated the contact angle of the aggregate with the solid surface and it was obtained a value of ≈75°.

It was also possible to analyze how the surfactant molecules arrayed with the rutile surfaces by calculating pair correlation functions $g(r)$. For this study we calculated the $g(r)$ of the CH_n groups with the titanium and oxygen atoms (of the TiO_2) in all the rutile surfaces (Fig. 11).

As a general feature we can observe that the CH_n groups were more structured with the atoms in the surface (1 0 0) than in the surface (0 0 1) as expected since surfactant molecules on the first surface seemed to array in well defined layers. However, the $g(r)$ of the CH_n with the TiO_2 in the surface (1 1 0) did not have strong peaks indicating that in this case the surfactant tails did not present much structure on the surface. These results were in agreement with those results obtained from the density profiles.

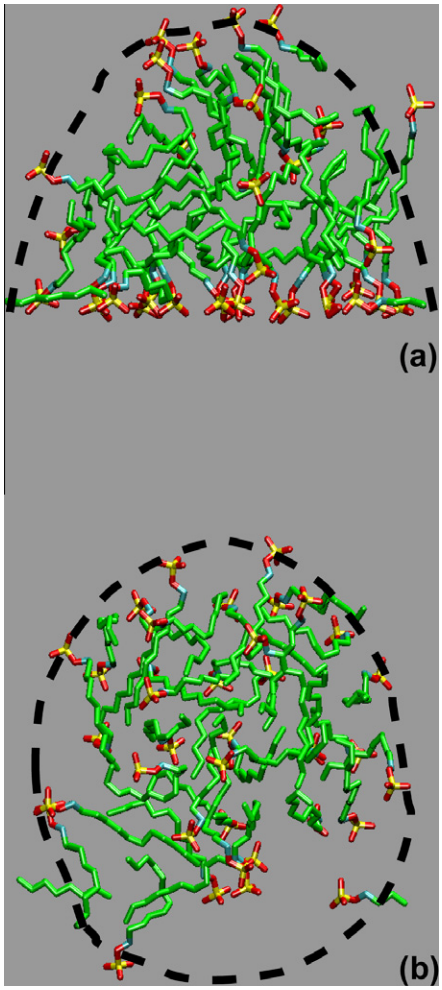

Fig. 10. Snapshot of surfactant molecules on the solid surface (1 1 0). (a) Snapshot in the *ZX* plane; (b) snapshot in the *XY* plane. The black dashed and continuous lines are a guide to see the approximated structure. The colors are the same as in Fig. 3. (For interpretation of the references to color in this figure legend, the reader is referred to the web version of this article.)

It is important to mention that here we have an inhomogeneous and nonsymmetric system in the z-direction, therefore, the $g(r)$ functions do not go to unity and they seem to take large values compared to the usual $g(r)$ of bulk systems.

Finally for the pair correlation function analysis we studied where water were located around the surfactant molecules. This study was conducted by calculating the $g(r)$ of the oxygens (in the water molecules) with the sulfur atoms (of the headgroup of the SDS molecules). In Fig. 12a we observed a peak near 4 Å for all the surfaces indicating that water solvated the headgroups, however, the number of waters around the headgroups (high of the peak) depended on the aggregated formed on the rutile surface. The position of the counterions (Na^+) with the SDS (sulfur atoms) was also evaluated in terms of the $g(r)$ function (Fig. 12b). The main peak was observed around 3.7 Å in all the systems at all rutile surfaces, nevertheless, we noted a shoulder at 3.2 Å on the left side of the first peak which corresponded to the closest contact between the sodium and sulfur atoms as other authors have previously reported [41–44], however, in our investigations this shoulder is more pronounced for the system with the surface (1 0 0).

3.3. Coverage

Since surfactant molecules might cover surfaces in different ways depending on the properties of the solid surfaces and of the solid–surfactant interactions an important parameter to study adsorption usually is the coverage. In the present work we measured coverage as the relation between the area occupied by all the atoms of the SDS molecules (in the tails and in the headgroups) in the first adsorbed layer (defined by molecules in the first peak of the density profile) with the total area of the surface.

In Figs. 13–15 the first adsorbed layers of all the systems are shown. In order to improve visualization these surfaces were duplicated in both *X*-axis and *Y*-axis. Moreover, in the figures some molecules look like incomplete since the figures show only atoms in the adsorbed layer.

Fig. 13 is the final configuration of the simulation carried out with the surface (0 0 1). In this case we observed that SDS molecules covered ≈ 60% of the solid surface. In Fig. 14 the final configuration of adsorbed molecules on the surface (1 0 0) is shown, where it was clear that hydrocarbon tails of the surfactant molecules were attached to the solid surface and a coverage of ≈ 72% was obtained. Besides, it was possible to see that surfactant molecules seemed to aggregate in an ordered structure.

Finally, for this study in Fig. 15 the final configuration of the first adsorbed layer of the system with the surface (1 1 0) is shown. Here, it was observed that some surfactant molecules were attached to the solid surface by their headgroups. In fact, for this orientation the coverage was 36% as a result of the low hydrophobicity of this surface orientation.

It is worthy to mention that in the solid surface (1 1 0) there were some sites which did not have surfactant molecules adsorbed suggesting that the interactions between the hydrophobic tails were stronger than those between the polar groups and the solid surface.

It was also possible to locate where the SDS molecules (of the first adsorbed layer) were attached on the surface by analyzing the number density profiles along the *Y* axis of the tails and headgroups of the SDS molecules and of the oxygen atoms in the TiO_2 surfaces. In Fig. 16a these profiles for the surface (1 0 0) are shown. The position of the oxygen atoms on the surface are depicted by the dashed lines and the SDS tails by the solid lines. We observed that the SDS tails (solid lines) were located between the oxygens, i.e. the profiles indicated that the tailgroups were adsorbed between the superficial oxygen atoms of the solid (see also Fig. 1b). For the surface (1 1 0), however, the headgroups (solid lines in Fig. 16b) were the groups located between the gaps of the upper oxygens on the surface (see Fig. 1c). For the surface (0 0 1) we did not observe any particular attachment of the SDS molecules on the surface.

3.4. Orientation and total length of hydrocarbon chains

These quantities can also give us insights of how molecules were arrayed to the different surfaces. Length of the hydrocarbon tails was measured by the distance from the last carbon to the first one closer to the headgroup, i.e. we calculated the average total length with the following equation;

$$\langle \mathbf{R} \rangle = \frac{1}{P}\frac{1}{N}\sum_{i=1}^{N,P} \Delta \mathbf{r}_i \tag{6}$$

N is the total number of SDS molecules, *P* is the number of configurations of the last 2 ns of simulation and

$$\Delta \mathbf{r}_i = \sqrt{(\Delta x)_i^2 + (\Delta y)_i^2 + (\Delta z)_i^2} \tag{7}$$

where Δx is the distance from the last to the first carbon atoms in the hydrocarbon chain in the *x* coordinate. Similar definitions are given for Δy and Δz. From these calculations we observed that lar-

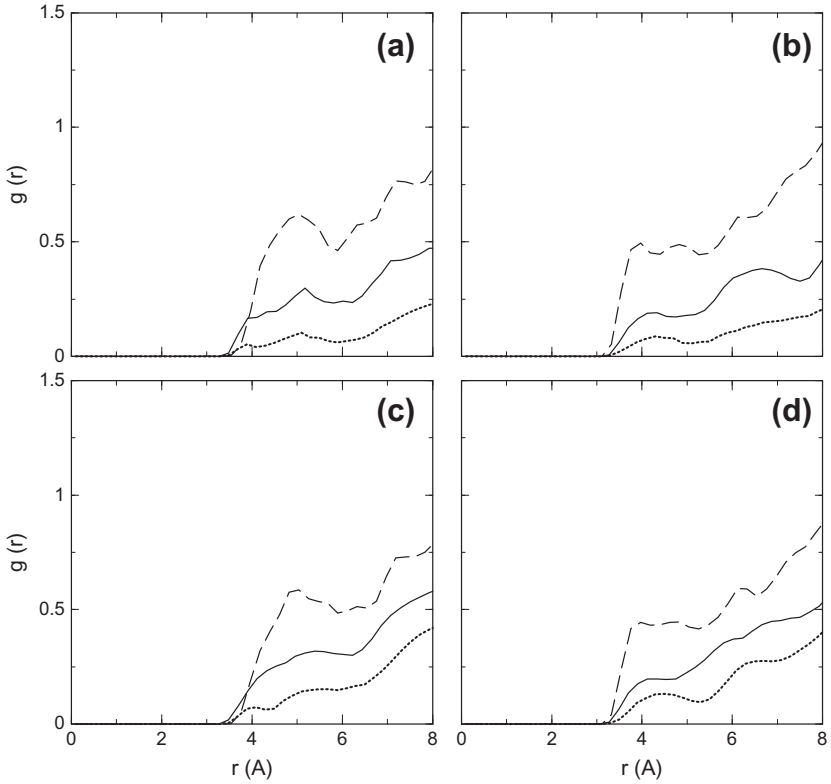

Fig. 11. $g(r)$ Functions of the CH_n groups (in SDS) with the titanium and oxygen atoms in the rutile surfaces (TiO_2). (a) $g(r)$ of $Ti(TiO_2)$–CH_3, (b) $g(r)$ of $O(TiO_2)$–CH_3, (c) $g(r)$ of $Ti(TiO_2)$–CH_2 and (d) $g(r)$ of $O(TiO_2)$–CH_2. The solid line is for the surface (001), the dotted line for the surface (110) and the dashed line for the surface (100).

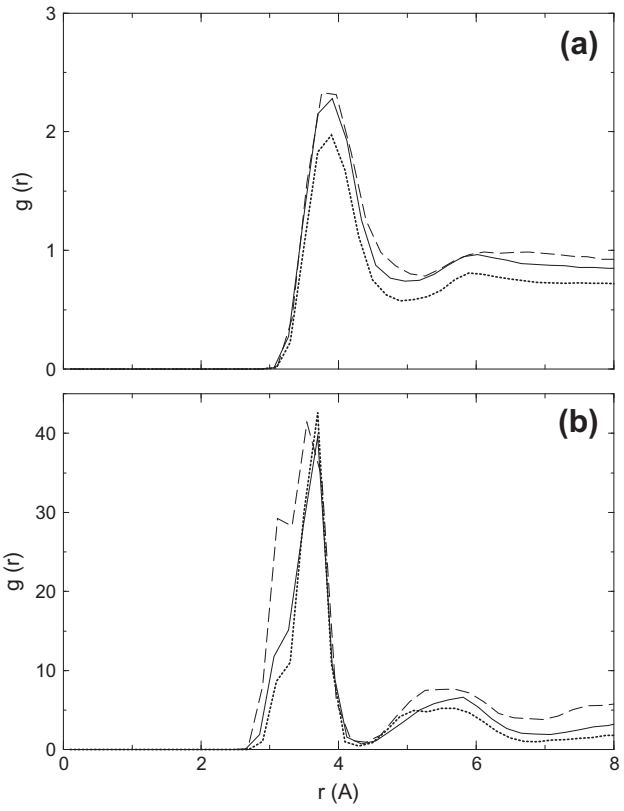

Fig. 12. $g(r)$ functions (a) of the sulfur atoms (in SDS) with the sodium atoms and (b) of the sulfur atoms (in SDS) with the oxygens in water. The solid line is for the surface (001), the dotted line for the surface (110) and the dashed line for the surface (100).

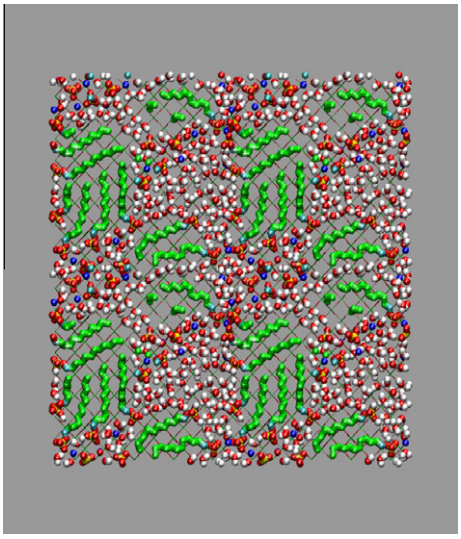

Fig. 13. Snapshot (*XY* plane) of the final configuration of the adsorbed molecules on the (001) surface. The colors are the same as in Fig. 3. (For interpretation of the references to color in this figure legend, the reader is referred to the web version of this article.)

ger tails were obtained on the surfaces (100) and (110) than on the surface (001) as shown in Table 4.

On the other hand, we calculated orientation of the hydrocarbon chains with respect to the vector normal to the interface by measuring the angle θ using the following equation;

$$\cos\theta_i = \left(\frac{\Delta z_i}{\Delta \mathbf{r}_i}\right) \tag{8}$$

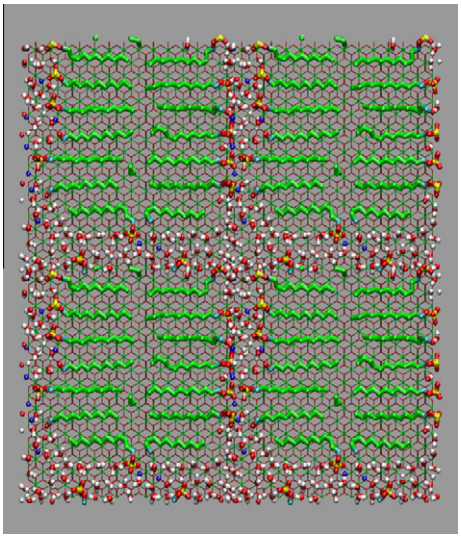

Fig. 14. Snapshot (*XY* plane) of the final configuration of the adsorbed molecules on the (100) surface. The colors are the same as in Fig. 3. (For interpretation of the references to color in this figure legend, the reader is referred to the web version of this article.)

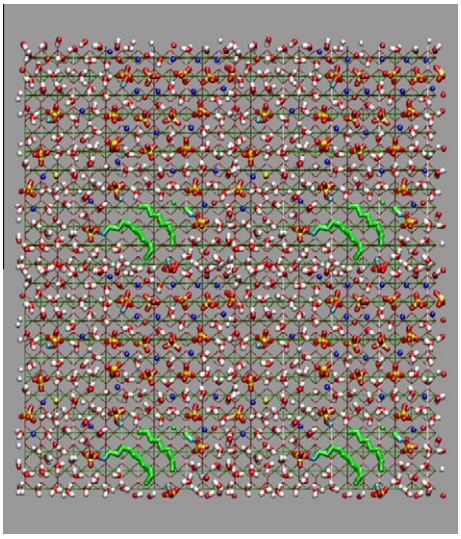

Fig. 15. Snapshot (*XY* plane) of the final configuration of the adsorbed molecules on the (110) surface. The colors are the same as in Fig. 3. (For interpretation of the references to color in this figure legend, the reader is referred to the web version of this article.)

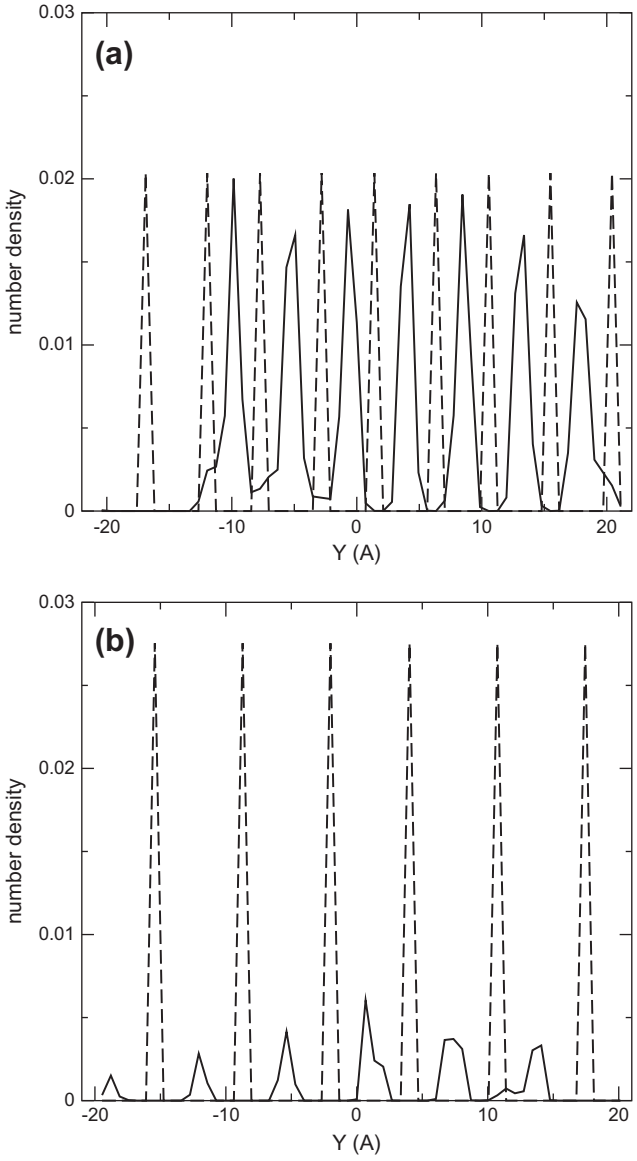

Fig. 16. Number density profiles in the *Y*-axis. for the surfactant molecules in the first adsorbed layer. (a) Surface (100). The dashed line corresponds to oxygen atoms in the surface and the solid line corresponds to hydrocarbon chains of the SDS molecules. (b) Surface (110). The dashed line corresponds to oxygen atoms in the surface and the solid line corresponds to the headgroup of the SDS molecules.

Table 4
Average total length of hydrocarbon chains in the three surface of rutile.

Plane	Total length (Å)
(001)	8.05
(100)	9.81
(110)	9.09

In Fig. 17 the angular distribution of the hydrocarbon chains with the surface (001) is shown where we observed a tendency of the tailgroups to be perpendicular to the vector normal to surface, i.e., several hydrocarbon chains were parallel to the solid surface. However, it was also possible to observe a peak around 55°, which indicated that molecules were not totally parallel to the solid surface.

In Fig. 18 we observed a high probability that the tails made an angle of 90° with the vector normal to the surface (100) indicating that most of the hydrocarbon chains were parallel to the solid surface. Finally, Fig. 19 suggests that SDS molecules aggregated on the surface (110) were not oriented in any preferred angle.

Not only we studied orientation of the surfactant tails but also we investigated how water molecules were oriented in the system. In Fig. 20 the angular distribution of the water dipole, respect with the vector normal to the interface, in different regions of the systems and in the different rutile surfaces is shown. Far from the solid plate, in the bulk phase, water had an uniform angular distribution in all the surfaces as expected (Fig. 20a). On the other hand, water slightly above the aggregate (but in the bulk phase) felt some influence of the surfactant molecules since it was possible to observe a small slope in the angular distribution of the dipole orientation (Fig. 20b). However, for water close to the

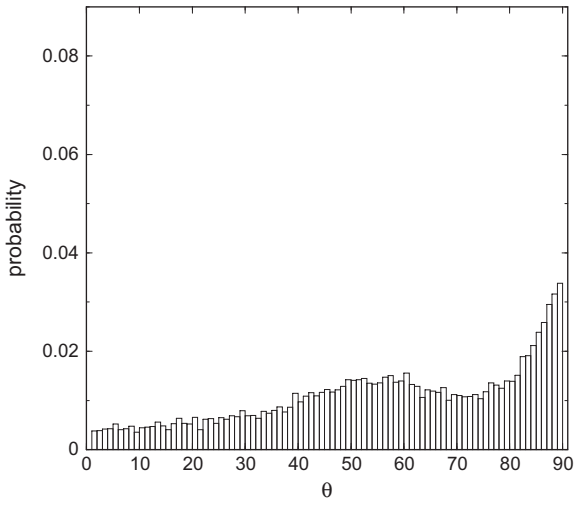

Fig. 17. Angular distribution of hydrocarbon chains with respect to the vector normal to the interface on the solid surface (001).

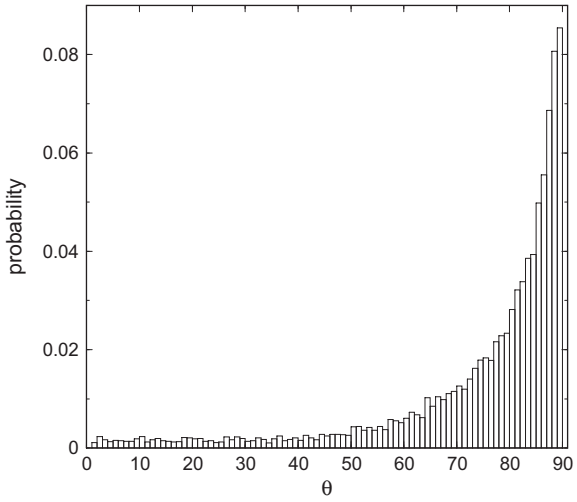

Fig. 18. Angular distribution of hydrocarbon chains with respect to the vector normal to the interface on the solid surface (100).

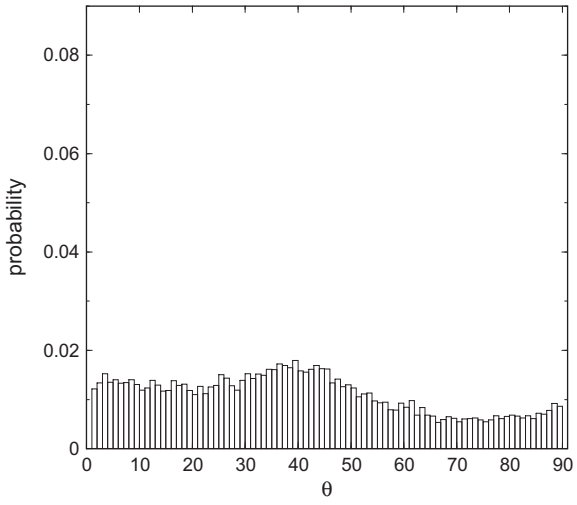

Fig. 19. Angular distribution of hydrocarbon chains with respect to the vector normal to the interface on the solid surface (110).

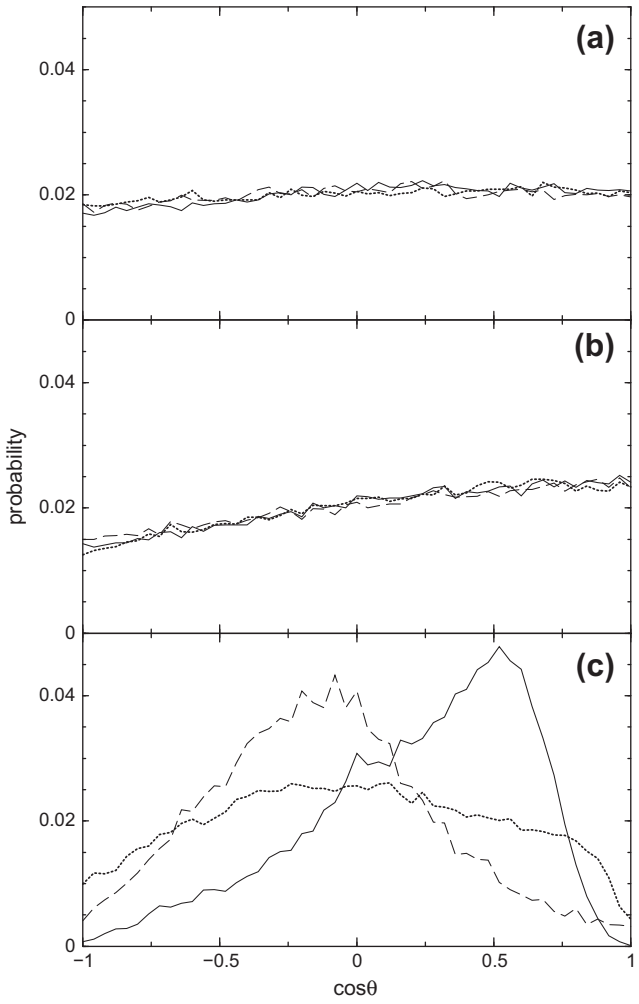

Fig. 20. Angular distribution of the water dipole vector (with respect to the vector normal to the interface) in different regions in the system and at the three rutile surfaces. (a) In the bulk phase, (b) just above the molecular aggregate and (c) on the surface of rutile. Solid line is for the surface (001), the dotted line for the surface (110) and dashed line for the surface (100).

surfaces (in the first adsorbed water layer calculated from the density profiles) different orientations were observed as shown in Fig. 20c. From that figure we noted that the surface (110) produced more uniform distribution of water on the surface whereas the surfaces (001) and (100) clearly showed an angular preference of water on the surface.

3.5. Order parameter

Finally, behavior of the tailgroups were also characterized in terms of the order parameter,

$$\mathbf{S}_{ij} = (1/2)\langle \cos\alpha_i \cos\alpha_j - \delta_{ij} \rangle \tag{9}$$

where $i, j = x, y, z$ and α is the angle between the ith molecular axis and the normal to the interface [45]. In this work it was more convenient to calculate the S_{zz} order parameter since this parameter gives us information about complete order parallel to the interface ($S_{zz} = -0.5$) or complete order in the direction normal to interface ($S_{zz} = 1.0$). In Fig. 21 the parameter S_{zz} is shown for each set of the surfactant molecules on the three different surface orientations.

As we observed, the results indicated that surfactant molecules on the surface (001) (long dashed line) have the some tails parallel to the interface whereas the tails on the surface (100) were mostly

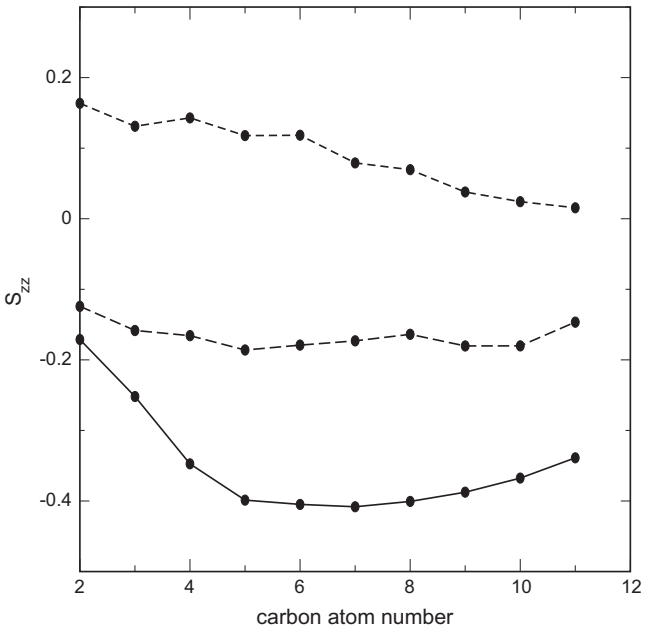

Fig. 21. The S_{zz} order parameter as a function of carbon position in the hydrocarbon chain of surfactants. Dashed line corresponds to surfactants on the surface (110), long dashed line is for the surfactants on the surface (001) and solid line corresponds to surfactants on the surface (100).

parallel to the solid surface (solid line). For the surface (100) the S_{zz} values did not suggest any preferred inclination of the tails in agreement with the results obtained from the angular distributions.

4. Conclusions and discussion

We performed a series of molecular dynamics computer simulations of an anionic surfactant (SDS) at three different rutile/water interfaces. Solid surfaces were built using different orientations of a crystalline cell, namely (001), (100) and (110) orientations.

We studied the structure of surfactant molecules on the rutile surfaces and from the density profiles differences and similarities on the SDS with the three different solid surfaces were depicted. While on the solid surface (110) the surfactant molecules were attached by their headgroups on the solid surfaces (001) and (100) the surfactant molecules were attached by the tailgroups. In fact, density profiles calculated in the surfaces (001) and (100) showed a structure of layers formed by hydrocarbon chains parallel to the surface indicated by the peaks in the profiles. However, in the system with the surface (110) it was not observed any layer structure.

When aggregate structures were analyzed it was observed that surfactant molecules on the surface (100) formed a hemicylinder shape similar to the structures reported in experiments of ionic surfactants on graphite [14] and in simulations of SDS on graphite [4]. On the other hand, surfactant molecules on the surface (110) were attached to the solid surface forming a structure which was approximated to a hemisphere. Even though surfactant molecules on the surface (001) had a similar behavior to that on the surface (100) in terms of layers formation on the solid surface it was not observed any regular molecular structure.

The sites of the solid surface on which the SDS molecules were adsorbed were also analyzed. It was found that the SDS molecules of the first layer on the surface (100) were adsorbed by the tailgroups and they were located between the superficial oxygen atoms of the surface. On the other hand, for the surface (110) adsorption was produced mainly by the headgroups which were deposited along the rows between the superficial oxygen atoms of the surface. However, in the case of the surface (001) we did not observe any tendency of the surfactants to be adsorbed in specific sites of the surface.

The differences in the aggregates formed on the three surface orientations can be explained in terms of the different solid structures. On the surface (110), half of the titanium cations are 5-fold coordinated while the remaining half are 6-fold coordinated as in bulk. On the other hand, the surface (100) has only 5-fold coordinated surface titanium atoms [46]. The slight difference between these two surfaces comes from the oxygen atoms on the (100) surface which are rotated 45° relative to those on the (110) surface. This difference implies that electrostatic interactions between the SDS headgroups and the titanium atoms are screened by the oxygen atoms in the surface (100).

Surface coverage was also studied and it was observed that the solid surface (110) had the smallest coverage, the surface (100) had the largest and the surface (001) had an intermediate coverage. Average total length of the tailgroups was also calculated and it was found that for surfactant molecules on the surfaces (001) and (110) the average length was smaller than that on the surface (100).

Orientation angles of the hydrocarbon chains with respect to the vector normal to the solid surface was calculated as a measurement of the affinity with the surfaces and it was found that for the system simulated on the surface (100) the angular distribution showed a peak close to 90° which indicated much affinity of the hydrocarbon chains with the solid surface. For the surface (001) it was also observed a small peak around 90°, however, in the case of the surface (110) it was not found any privileged angle, i.e. the distribution showed several angles suggesting that the tailgroups were not completely attached to the solid surface.These results were in agreement with the order S_{zz} parameter calculations.

Orientation of the surfactant tails and aggregation on the surface (110) suggested adsorption of the molecules were related with the electrostatic interactions between the SDS polar groups and titanium atoms exposed on the solid surface. In fact, there was a peak in the density profile for water close to the peak of the headgroups which suggested that this surface was not as hydrophobic as surfaces (100) and (001).

Finally, as far as we know aggregates on titanium dioxide have not been studied from a structural point of view. In fact, from the present investigations we studied the importance of solid structures interacting with surfactant molecules, in order to determine the formation of aggregates on the surface of the solid. Therefore, from these studies we obtained more insights about the influence on surfactant molecules adsorbed by three different solid surfaces built from a single crystal.

Acknowledgments

We acknowledge support from DGAPA-UNAM-Mexico through Grant IN102207 and DGTIC-UNAM for the Kanbalam supercomputer facilities. ENR acknowledges the scholarship and support from CONACyT Mexico.

References

[1] M. Ahmaruzzaman, D.K. Sharma, J. Colloid Interface Sci. 287 (2005) 14.
[2] A. Bhatnagar, A.K. Jain, J. Colloid Interface Sci. 281 (2005) 49.
[3] I.F. Uchegbu, A.G. Schtzlein, Polymers in Drug Delivery, CRC Press. Taylor and Francis Group, LLC, 2006.
[4] M. Sammalkorpi, A.Z. Panagiotopoulos, M. Haataja, J. Phys. Chem. B 112 (2008) 2915.
[5] Guannan Mu, Xianghong Li, J. Colloid Interface Sci. 289 (2005) 184.
[6] A.M. Gaudin, D.W. Fuerstenau, Trans. Am. Inst. Min. Metall. Pet. Eng. 202 (1955) 66.
[7] M.R. Bhömer, L.K. Koopal, Langmuir 8 (1992) 2649.

[8] D.W. Fuerstenau, J. Phys. Chem. 60 (1956) 981.
[9] Z. Király, G.H. Findenegg, J. Phys. Chem. B 102 (1998) 1203.
[10] J. Penfold, E.J. Staples, I. Tucker, L.J. Thompson, Langmuir 13 (1997) 6638.
[11] F. Tiberg, B. Joensson, B. Lindman, Langmuir 10 (1994) 3714.
[12] P. Chandara, P. Somasundaranan, N.J. Turro, J. Colloid Interface Sci. 117 (1987) 31.
[13] W.A. Ducker, E.J. Wanless, Langmuir 12 (1996) 5915.
[14] S. Manne, J.P. Cleveland, H.E. Gaub, G.D. Stucky, P.K. Hansma, Langmuir 10 (1994) 4409.
[15] H.N. Patrick, G.G. Warr, S. Manne, I.A. Aksay, Langmuir 13 (1997) 4349.
[16] M. Jaschke, H.J. Butt, H.E. Gaub, S. Manne, Langmuir 13 (1997) 1381.
[17] W.A. Ducker, E.J. Wanless, J. Phys. Chem. B 100 (1996) 3207.
[18] H. Schniepp, H. Shum, D. Saville, I. Aksay, J. Phys. Chem. B 111 (2007) 8708.
[19] E. Topoglidis, C.J. Campbell, A.E.G. Cass, Langmuir 17 (2001) 7899.
[20] S.R. Whaley, D.S. English, E.L. Hu, P.F. Barbara, A.M. Belcher, Nature 405 (2000) 665.
[21] K. Esumi, K. Sakai, K. Torigoe, T. Suhara, H. Fukui, Colloids Surf. A: Physicochem. Eng. Aspects 155 (1999) 413.
[22] S. Fukushima, S. Kumagai, J. Colloid Interface Sci. 42 (1973) 539.
[23] K. Esumi, A. Toyoda, M. Goino, T. Suhara, H. Fukui, Y. Koide, J. Colloid Interface Sci. 202 (1998) 377.
[24] N.H. Tkachenko, Z.M. Yaremko, C. Bellman, M.M. Soltys, J. Colloid Interface Sci. 299 (2006) 686.
[25] A. Heller, Acc. Chem. Res. 28 (1995) 503.
[26] M.R. Hoffmann, S.T. Martin, W. Choi, D.W. Bahnemann, Chem. Rev. 95 (1995) 69.
[27] M. Ramamoorthy, D. Vanderbilt, Phys. Rev. B 49 (1994) 16721.
[28] S. Horikoshi, D. Minami, Seya Ito, H. Sakai, D. Kitamoto, M. Abe, N. Serpone, J. Photochem. Photobiol. A: Chem. 217 (2011) 141.
[29] R. Wang, N. Sakai, A. Fujishima, T. Watanabe, K. Hashimoto, J. Phys. Chem. B 103 (1999) 2188.
[30] F. Zheng, X. Zhang, W. Wang, W. Dong, Langmuir 22 (2006) 11214.
[31] K. Shah, P. Chiu, M. Jain, J. Fortes, B. Moudgil, S. Sinnott, Langmuir 21 (2005) 5337.
[32] H. Dominguez, J. Phys. Chem. B 111 (2007) 4054.
[33] H.J.C. Berendsen, J.R. Grigera, T.P. Straatsma, J. Phys. Chem. B 91 (1992) 6269.
[34] J.R. Lu, A. Marroco, T.J. Su, R.K. Thomas, J. Penfold, J. Colloid Interface Sci. 174 (1993) 441.
[35] H. Dominguez, A. Gama Goicoechea, N. Mendoza, J. Alejandre, J. Colloid Interface Sci. 297 (2006) 370.
[36] H. Dominguez, J. Phys. Chem. B 106 (2002) 5915.
[37] T.R. Forester, W. Smith, DL-POLY Package of Molecular Simulation, CCLRC, Daresbury Laboratory: Daresbury, Warrington, England, 1996.
[38] W.G. Hoover, Phys. Rev. A 31 (1985) 1695.
[39] J.P. Ryckeart, A. Bellemans, A. Chem. Phys. Lett. 123 (1975) 30.
[40] H. Domínguez, Langmuir 25 (2009) 9006.
[41] C.D. Bruce, M.L. Berkowitz, L. Perera, M.D.E. Forbes, J. Phys. Chem. B 106 (2002) 3788.
[42] N.R. Tummala, A. Striolo, J. Phys. Chem. B. 112 (2008) 1987.
[43] N.R. Tummala, A. Striolo, Phys. Rev. E. 80 (2009) 021408.
[44] H. Dominguez, J. Colloid Interface Sci. 345 (2010) 293.
[45] H.J.C.E. Egberts, J. Berendsen, J. Chem. Phys. 89 (1988) 3718.
[46] V.E. Henrich, R.L. Kurtz, Phys. Rev. B 23 (1981) 6280.